energies

MDPI

Article

Seamless Transition and Fault-Ride-Through by Using a Fuzzy EO PID Controller in AVR System

Ahmed O. Badr [1], Soha Mansour [1], Mariam A. Sameh [2,*] and Mahmoud A. Attia [1]

[1] Electrical Power and Machines Department, Faculty of Engineering, Ain Shams University, Cairo 11566, Egypt
[2] Electrical Engineering Department, Faculty of Engineering, Future University in Egypt, Cairo 11835, Egypt
* Correspondence: mariam.ahmed@fue.edu.eg

Abstract: One of the most crucial control aspects in electric power networks is ensuring constant voltage levels throughout different circumstances. To overcome this problem, an automatic voltage regulator (AVR) is installed in the electrical power networks to preserve the voltage at its allowable range. In this paper, a fuzzy-based PID controller was used to enhance the AVR dynamic performance under several operating conditions. Moreover, an Equilibrium Optimizer (EO) algorithm was used to initialize the controller gains. The validation of the proposed controller was proven through three different systems. The first was a simple AVR system under fixed and dynamic references. The proposed fuzzy EO PID controller proved its superiority in this case through the reduction of voltage overshoot by around 3–28% compared with the reported methods in the literature. Then, the fault-ride through capability of the proposed controller was proven through the second system, which was the Kundur two-area system suffering from a 3-phase fault condition, where the overshoot with the proposed controller was reduced by 4–7% compared with the default controller and modern weighted method reported in the literature. Lastly, an IEEE 9-bus system performance was tested with the proposed controller under normal, faulty, and dynamic loading conditions. Again, the proposed controller succeeded in reducing the maximum overshoot by around 5% compared with the default controller in the system. Moreover, the proposed controller achieved a seamless transition between the islanding and grid-connected mode of operation.

Keywords: fault ride through; automatic voltage regulator; fuzzy logic; PID controller; equilibrium optimizer; optimization

check for updates

Citation: Badr, A.O.; Mansour, S.; A. Sameh, M.; Attia, M.A. Seamless Transition and Fault-Ride-Through by Using a Fuzzy EO PID Controller in AVR System. *Energies* **2022**, *15*, 8475. https://doi.org/10.3390/en15228475

Academic Editor: Mario Marchesoni

Received: 17 September 2022
Accepted: 3 November 2022
Published: 13 November 2022

Publisher's Note: MDPI stays neutral with regard to jurisdictional claims in published maps and institutional affiliations.

Copyright: © 2022 by the authors. Licensee MDPI, Basel, Switzerland. This article is an open access article distributed under the terms and conditions of the Creative Commons Attribution (CC BY) license (https://creativecommons.org/licenses/by/4.0/).

1. Introduction

A deviation in grid voltage such as voltage sag or swell may lead to significant changes in the dynamics of the power system, which will adversely affect the power quality of the power grid, the reliability, and the security of the power system. Consequently, the electric equipment that is connected to the network will suffer from deteriorated performance as they are supposed to work at a certain voltage level. Furthermore, controlling the bus voltage impacts the reactive power, thus making it possible to decrease the line losses as the reactive current component will be regulated. Moreover, voltage disturbances can affect the reactive power sharing, which will influence the parallel operation of the generation units. These events can lead to unstable power system operations, which will eventually lead to severe financial problems. Thus, an AVR system is used to maintain the output voltage of the synchronous generator at its nominal value and reduces its variation under abnormal system situations such as fault and different loading conditions. The basic operation of the AVR is to control the DC field excitation current of the exciter connected to the rotor of the synchronous generator in response to the change in the terminal voltage. Accordingly, the induced voltage across the stator of the synchronous generator will be sustained [1–5].

To realize the AVR goals, an effective controller must be utilized to reach the predetermined voltage level with a fast response considering the improved performance of

both large- and small-signal stability. A proportional integral derivative (PID) controller is usually employed in most applications due to its simple structure, easy realization, low cost, and satisfactory performance [5]. A PID controller typically is a combination of three fundamental parameters, namely proportional gain, integral gain, and derivative gain. Precise tuning of these coefficients is required to achieve robust and reliable system performance [6]. Generally, we can divide these tuning methods into two main categories: classical and optimization methods.

Classical methods include the Ziegler–Nichols, model matching, and Cohen–Coon techniques. Frequency domain and phase-margin design approaches are also considered classical. The main disadvantage of these methods is that they rely on trial and error. Moreover, due to the complexity and non-linearity of the power system, varying operating points, and high field winding inductance of the generator classical tuning methods of PID function mainly assume linear systems fail to achieve the appropriate requirements.

Accordingly, heuristic optimization methods have been considered to tune the gains of the PID controllers to yield stable and robust performance of the AVR [7]. Authors of [1] used the symbiotic organisms search (SOS) algorithm to tune the PID controller of the AVR system, they found that the controller performance enhanced in time and frequency domains. Authors of [2] used a local unimodal sampling method to tune AVR system PID gains, they found the system was enhanced through settling time and overshoot reduction. Authors of [3] used harmony search, local unimodal sampling, and teaching–learning-based methods to tune the AVR controllers, two types of controllers were used in this paper. The authors used integrated square error as an objective function and found that the PID-Accelerated controller was superior to the PID. Authors of [4] used the D-decomposition method to enhance the AVR system performance. The authors of this paper found the design strength of their methodology is that it takes into account three control concerns at the same time, which are optimization of performance, robust stability, and the resiliency of the controller. In [8], the PID coefficients were obtained using the particle swarm optimization (PSO) technique. In [9], the authors utilized the PSO algorithm to get the optimum gains of a high-order AVR PID controlled by applying a new cost function to acquire a lower number of iterations and rapid convergence of PID gains. Ekinci and Hekimoglu used an improved kidney-inspired algorithm (IKA) in [10] to optimally evaluate the PID gains of the AVR system, they provided a comparative analysis for the transient behavior of the system with numerical simulations. A fractional-order PID was designed in [11] where the multi-objectives extremal optimization algorithm (MOEO) was used for three objective functions based on the integral of absolute error. In [12], Bingul and Karahan, based on the time-domain characteristics of AVR terminal voltage (maximum overshoot, steady-state error, and settling time), proposed a new objective function. The authors tested their function with the artificial bee colony (ABC), cuckoo search (CS), and PSO algorithms and they found that the best robustness against parametric uncertainties was achieved with the CS technique. Another study motivated by the FIFA World Cup, introduced a meta-heuristic optimization method to tune the PID coefficients. They compared their work with PSO and the genetic algorithm (GA) and concluded that World Cup Optimization (WCO) showed better performance [13]. The tree-seed algorithm (TSA) was introduced in [5] to fine-tune the gains of the PID controller in an AVR system. According to their analysis, the TSA showed exceptional steady state and transient responses over other techniques such as PSA, ABC, and IKA. The application of the fractional order PID (FOPID) controller while applying chaotic ant swarm [14] and improved evolutionary non-dominated sorting genetic algorithms (NSGA-II) [15] have been also applied to solve the AVR control problem. The FOPID controller possesses two extra parameters than the standard PID controller, allowing us to have more degrees of freedom while using the FOPID controller but at the expense of adding more complexity to the system. In [16], Gozde and Taplamacioglu used the ABC algorithm to calculate the optimum PID gains. The results were compared with PSO and the differential evolution (DE) algorithm in different areas such as root locus, bode diagram, and transient studies.

They concluded that ABC gave optimal performance regarding the transient behavior of the terminal voltage. In [17], the author applied the whale optimization algorithm (WOA) for both PID and PID-Accelerated (PIDA) controllers. The PIDA controller revealed better performance than the PID controller. WOA was also used in [18] to optimize the gains of PID, and PID plus second-order derivative (PIDD2) controllers. The PIDD2 controller showed more reliable performance by adding WOA among other techniques. Teaching–learning-based optimization (TLBO) was conducted in [19] to acquire the optimization of the PID controller while in [3] the authors compared three techniques, which are the harmony search algorithm (HSA), TLBO, and local unimodal sampling (LUS) in tuning the gains of the PID and accelerated PID (PIDA) controllers. The PIDA controller was proven to have better stability and transient behavior than the PID controller. The authors in [20] applied the equilibrium optimizer (EO) method to determine the most appropriate PID controller gains in an AVR system. The EO technique showed excellent performance in terms of convergence speed and accuracy. As the authors claimed in [21], the future search algorithm (FSA) proved to have superior performance when used to tune the gains of the PID controller of the AVR system.

Despite the numerous heuristic self-tuning optimization techniques, there are still many difficulties imposed on the control system of the AVR due to the non-linearity and uncertainty of the power system. Also, variable operating power system states and several kinds of system disturbances require a flexible PID control structure to achieve the required fast stable and reliable performance of the system. Fuzzy logic controllers have been developed to incorporate the power system nonlinearity and complexity into the controller model to improve the overall system performance. For instance, in [22] the authors used a fuzzy-based PID controller (FP+FI+FD) to preserve the terminal voltage level of the generator at its predetermined value and the gains of fuzzy PID have been tuned by a hybrid of PSO and GA (HGAPSO) to add more robustness to the system. In [23], a fuzzy-based PID controller was used, and the gains were optimized by TLBO. In [24], a discrete fuzzy PID controller was introduced to control the AVR of a single machine infinite bus model (SMIB), which showed better damping properties. In [25], CRPSO was used for the offline tuning of PID while Sugeno fuzzy logic (SFL) was utilized for the online operating conditions. This technique gave less computational burden than a binary-coded GA SFL PID controller. An interval type 2 fuzzy PID-based controller has been presented in [26] where outstanding transient and steady-state performance was monitored

In this paper, the objective was to enhance the AVR system performance and capabilities. For this goal, a fuzzy-based PID controller was auto-adopted for the control of the AVR system. In addition, the EO algorithm was employed to initialize the gains of the PID controller to achieve higher disturbance rejection and decrease the fuzzy system computational burden. The proposed controller was applied to the Kundur two-area system and IEEE 9-bus system to prove its reliability and robustness. Moreover, the fault-ride-through and seamless transition capabilities were tested through case studies. Furthermore, the proposed controller covered the gap in the literature by having dynamic controller gains that can be auto-adapted to deal with different types of disturbances that they were not designed for.

2. System Modelling

Three different models were considered in this paper. The first one was the simple AVR model, the second model was the Kundur two-area system, and the final model was the IEEE 9-bus system.

2.1. Automatic Voltage Regulator (AVR) System

Automatic voltage regulator (AVR) is an effective device used for adjusting and regulating the output voltage of a synchronous generator within its nominal value under all loading conditions. Figure 1 shows the main components of the AVR system [3]. The controller gains are harnessed to control the excitation current of the synchronous generator.

The output current of the generator is measured by the sensor and compared with its reference value to allow the error to be processed by the controller to give the suitable action to the exciter of the generator through the amplifier. The amplifier is used to convert the controller signal into a suitable controlling signal for the exciter [3]. The controller used in this study was the fuzzy-based PID controller with an EO algorithm to initialize the PID gains.

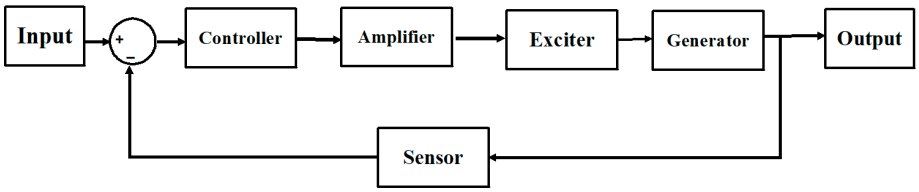


Figure 1. Block diagram of AVR System.

These gains were optimized for minimum sum and integral square of error, where the objective function is given in Equation (1):

$$F_O(\text{ISE}) = \sum error^2 \tag{1}$$

The transfer functions of the amplifier, exciter, generator, and sensor are given by Equations (2)–(5). While the ranges and set values for their gains are given in Table 1 [3].

$$TF_a = \frac{A}{a+1} \tag{2}$$

$$TF_e = \frac{E}{e+1} \tag{3}$$

$$TF_g = \frac{G}{g+1} \tag{4}$$

$$TF_s = \frac{S}{s+1} \tag{5}$$

Table 1. Range and set values for gains.

Symbol	Range	Set Value
A	$10 \leq A \leq 40$	10
a	$0.02 \leq a \leq 0.1$	0.1
E	$1 \leq E \leq 10$	1
e	$0.4 \leq e \leq 1$	0.4
G	$0.7 \leq G \leq 1$	1
g	$1 \leq g \leq 2$	1
S	$0.7 \leq S \leq 1$	1
s	$0.001 \leq s \leq 0.06$	0.01

2.2. Kundur System

The Kundur system, also known as the two-area system was first developed by Prabha Kundur in 1994 [27]. The system connects two areas through a double transmission line of 220 km each at 230 kV, connecting the two buses B1 and B2. At each bus, a load and a capacitor are connected in parallel, as shown in Figure 2 [28]. The load is distributed such that the tie line power from area 1 to area 2 is 413 MW while the capacitors at each area are rated 187 MVAr. It is assumed that the two areas are similar, and each one is made up of two coupling units. The Kundur system is used as a standard system for the

dynamic study of transmission systems [28]. Each area consists of 2 identical generators rated 20 kV/900 MVA with an AVR system based on a lead–lag controller. The system suffers from a 3-phase fault in the middle of TL1 at t = 1 sec and cleared after 12 cycles.

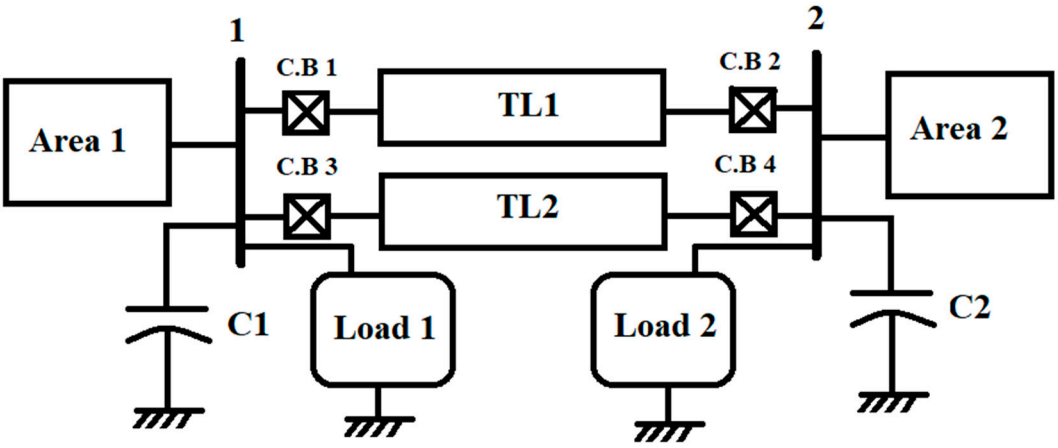


Figure 2. Block diagram of Kundur system.

2.3. IEEE 9-Bus System

The IEEE standard systems are commonly used by researchers and students worldwide. They are quite effective to study any new problem or test any new methodology since it is quite difficult to have real system data available for all researchers. The IEEE 9-bus system is relatively popular since it is simple and all-encompassing. It includes nine buses, three of them are generation buses and three are load buses. The remaining three buses are connecting buses. A single-line diagram for the standard IEEE 9-bus system is given in [29]. The generator at bus 1 is rated at 10,000 MVA/16.5 kV, acting as the grid, whereas the generators at buses 2 and 3 are rated 200 MVA/13.8 kV each with an AVR controller. The interconnecting lines between all generators operate at 230 kV. The loads of the systems L1, L2, and L3 are 100 MW/35 MVAr, 125 MW/50 MVAr, and 90 MW/30 MVAr, respectively.

3. Fuzzy EO PID Controller

Fuzzy control systems were introduced as a new paradigm for automatic control following the development of fuzzy sets by L.A.Zadeh in 1965. A fuzzy controller can be considered as a nonlinear controller defined by linguistic rules such as big and small instead of differential equations. Accordingly, a fuzzy system can handle systems that include deficient, vague, uncertain, or imprecise information without considering the mathematical model of the system [30]. Fuzzy logic introduces the concept of an infinite number of truth values mapped between 0 and 1, unlike classical logic which has only two truth values 0 or 1. A fuzzy logic controller is composed of three fundamental stages [30–33].

3.1. Fuzzification Stage

This stage is responsible for the transformation of the inputs from crisp values to linguistic variables using different kinds of membership functions stored in the knowledge base. Each crisp input is assigned a degree to the fuzzy subset they belong via the membership function.

3.2. Inference Mechanism and Rule Knowledge Base

This is the decision-making stage where the fuzzy inputs are mapped into fuzzy decisions using a set of linguistic if-then rules that are stored in the fuzzy rule base. The implication is applied using logical operators such as AND (min) and OR (max) to achieve a consequent out of the antecedent. The antecedent is a weighted fuzzy input with a single number whereas the consequent is a fuzzy set reshaped by a membership function. Aggregation is then employed to combine the output consequent of each fuzzy rule into one

fuzzy set. Several methods are used for aggregation such as maximum, and probabilistic OR. The most famous inference mechanisms to draw out a conclusion from fuzzy knowledge are the Mamdani and Sugeno models. The main difference between these two inference engines is in the output stage where the Mamdani model has an output membership function whereas the Sugeno model uses a weighted average of the consequents which are no longer fuzzy sets but mostly linear formulas to compute the output.

3.3. Defuzzification

This stage is the process of obtaining a non-fuzzy crisp from the output from the aggregate fuzzy set to be processed as a control signal. Various defuzzification methods exist, such as the centroid average, maximum center average, bisector, and largest of maximum. The fuzzy inference process diagram is shown in Figure 3.

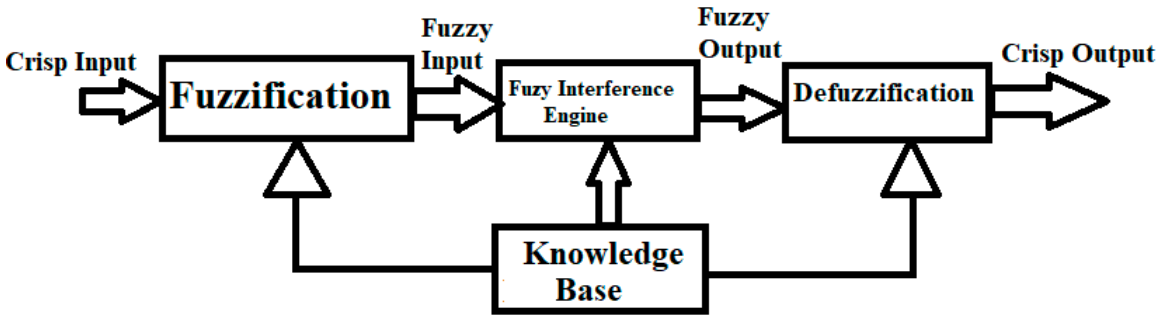


Figure 3. Fuzzy inference process diagram.

In our system, a fuzzy logic controller (FLC) was added in series with the conventional PID controller where the output of the fuzzy controller was taken as an input to the conventional PID. Two inputs were used for the FLC, which were the error between the reference voltage and the actual terminal voltage of the generator, and the derivative or change of the error. In this manner, the input to the PID was continuously altered based on the fuzzy rules, which resulted in an online auto-tuned signal to the PID controller to cope with any change in the AVR system to acquire a better dynamic and steady-state response. Moreover, the EO optimization was used to initialize the gains of the PID controller. The membership function of the proposed fuzzy logic controller is shown in Figure 4, with 25 rules shown in Table 2 [33].

Table 2. Rules for the proposed controller [33].

		Error				
		NB	N	Z	P	PB
Change of error	NB	NB	NB	NB	N	Z
	N	NB	NB	N	Z	P
	Z	NB	N	Z	P	PB
	P	N	Z	P	PB	PB
	PB	Z	P	PB	PB	PB

Where NB, N, Z, P, and PB are Negative Big, Negative, Zero, Positive, and Positive Big, respectively.

The fuzzy consequents were generated from the antecedents using the minimum-type implication method. Then the output fuzzy set for each case was obtained using the maximum-type aggregation method. The control signal that will be applied to the AVR system to adjust the voltage error was then produced using the centroid method of defuzzification. The inference engine incorporated the Mamdani fuzzy model. The fuzzy controller used in this paper was type 1 and called T1FLC (type-1 fuzzy logic controller), as shown in Figure 5.

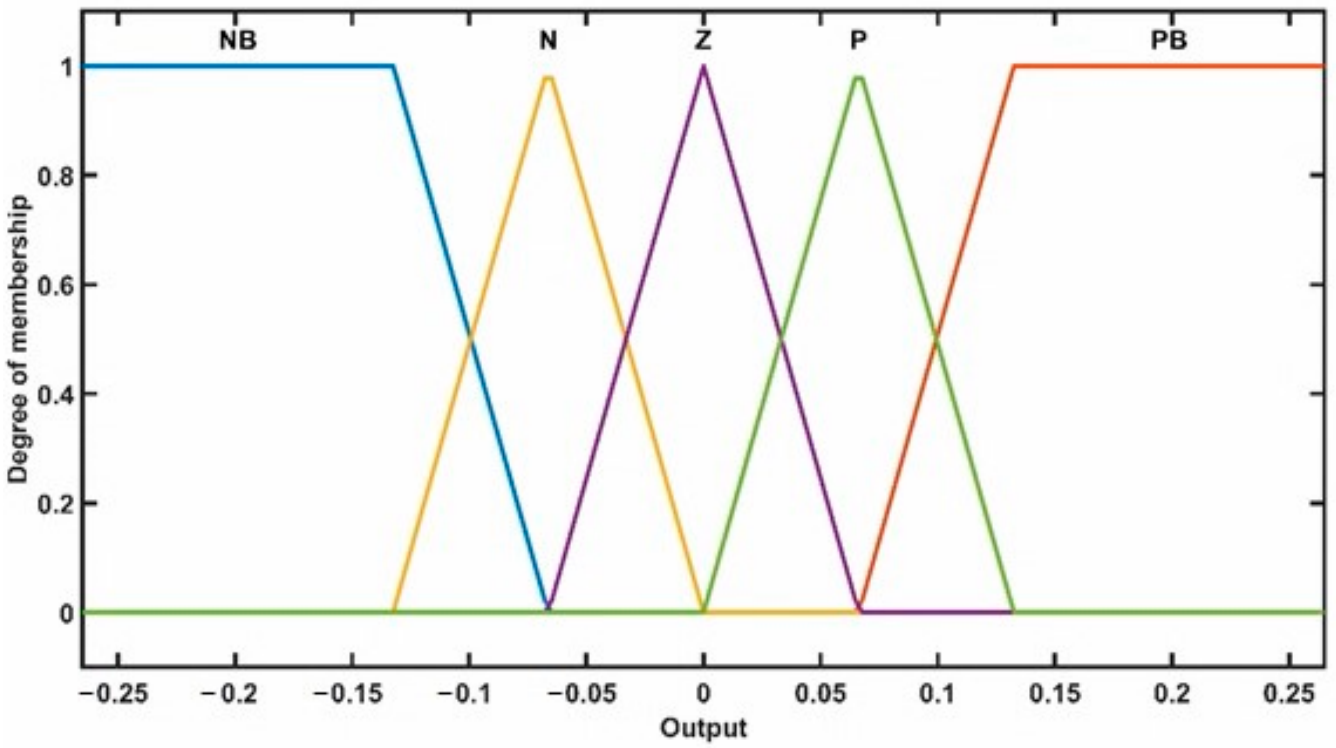


Figure 4. Output membership function.

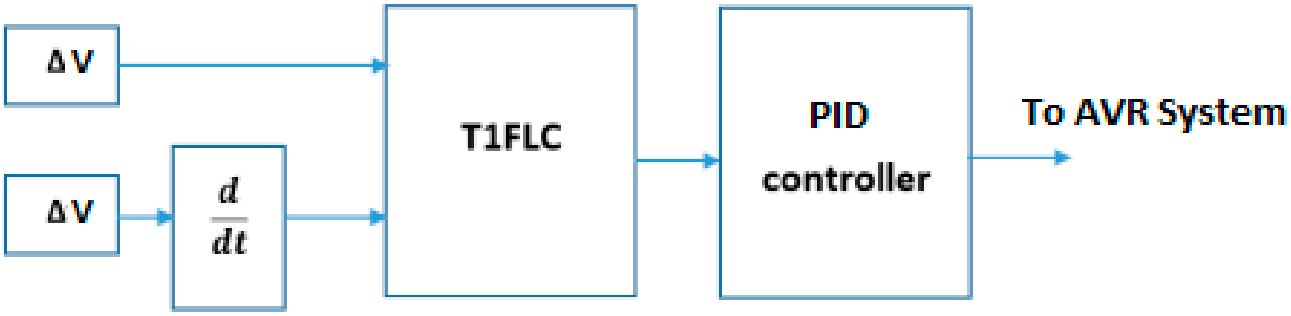


Figure 5. The fuzzy control system diagram.

4. Equilibrium Optimizer (EO)

In 2020, Afshin Faramarzi introduced a new optimization algorithm named the "Equilibrium Optimizer" algorithm (EO) [34]. Faramarzi was inspired by this algorithm by the balance models of control between volume and mass, which is used for the estimation of dynamic and equilibrium states. As usually known in most metaheuristic algorithms, a population of candidate solutions is initially generated, then a specified function is used for updating the candidate solutions in each iteration. This specified function differs from one algorithm to another according to the attitude of the animal or rule that inspired the algorithm. For the EO, the concentration term K is calculated for each candidate solution for iteration updates. K can be calculated from Equation (6).

$$\vec{K} = \vec{K_{eq}} + (\vec{K} - \vec{K_{eq}})\,\vec{J} + \frac{\vec{g_r}}{\delta U}\left(1 - \vec{J}\right) \quad (6)$$

Given that,
K is the concentration inside the volume;
U is the volume;

K_{eq} is the concentration at an equilibrium state;
g_r is the mass generation rate;
δ is the turnover rate, it is assumed to be a random vector in the interval of [0, 1];
And To is the initial start time.
While $\vec{J}$ can be calculated from Equation (7)

$$\vec{J} = c_1 \text{ sign } \left(\vec{\rho} - 0.5\right) \left[e^{-\vec{\delta}\ T} - 1\right] \tag{7}$$

Known that,
c_1 & c_2 are constant values that control exploration ability, hey are equal to 2 and 1 respectively; and
ρ is a random vector in the interval of [0, 1].
Moreover, T is time defined as a function of the current iteration (It), maximum number of iterations (It_m), and decreases with the number of iterations. It can be determined from Equation (8).

$$\mathrm{T} = \left(1 - \frac{\mathrm{It}}{It_m}\right)^{\left(c_2 \frac{\mathrm{It}}{It_m}\right)} \tag{8}$$

where, g_r can be determined from Equation (9), while g_{ri}, To, and $p(g)$ are calculated from Equations (10)–(12), respectively.

$$\vec{g_r} = \vec{g_{ri}}\, e^{-\vec{\delta}(T - T_o)} = \vec{g_{ri}}\ \vec{J} \tag{9}$$

$$\vec{T_o} = \frac{1}{\delta} \ln\left(-c_1 \text{ sign } \left(\vec{\rho} - 0.5\right)\left[1 - e^{-\delta\ T}\right]\right) + \mathrm{T} \tag{10}$$

$$\vec{g_{ri}} = \vec{C}_p \left(\vec{K_{eq}} - \vec{\delta}\ \vec{K}\right) \tag{11}$$

$$\vec{C}_p = \begin{cases} 0^{0.5\rho_1} & \rho_2 \geq p(g) \\ & \rho_2 < p(g) \end{cases} \tag{12}$$

Note that,
ρ_1 & ρ_2 are random numbers in the interval of [0, 1];
C_p is a vector constructed by the repetition; and
$p(g)$ is the generation probability.
EO was used to initialize the PID gain of the proposed fuzzy EO PID controller, and the flowchart in Figure 6 shows how it was used in this case [34]. The EO parameters setting in this study was as follows: the maximum number of iterations was 100, with 3 dimensions, and 5 particles.

According to [3], there are different objective functions, such as the integral of square error (ISE), integral of absolute error (IAE), and integral of time-weighted square error (ITSE). Due to the equal weighting of all errors, ISE and IAE have minimal maximum overshoot (Mp) and long settling times (Ts) (time-independent). Although ITSE solves this issue, it is time-consuming and requires difficult analytical formulas. Thus, we used ISE in this work.

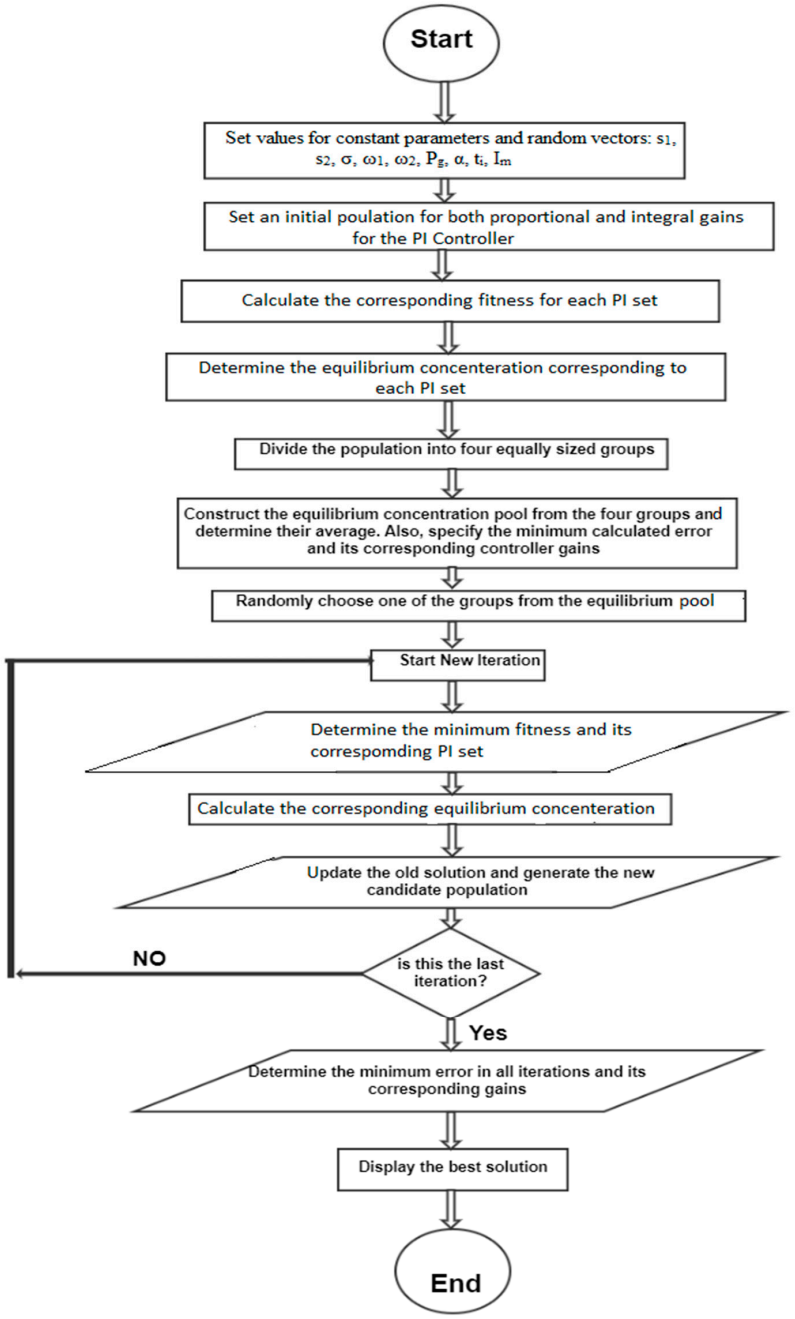


Figure 6. Flow chart of EO algorithm.

5. Results and Discussion

Three cases will be studied in this paper. The first case is an examination of the proposed controller through a simple AVR model, shown in Figure 1. While the second and third cases are robustness tests of the proposed controller in the Kundur and IEEE 9-bus systems. The IEEE 9-bus system is studied under normal, faulty, and dynamic loading conditions. Moreover, the proposed controller is used to achieve a smoothing transition between the islanding and grid-connected modes of operation. For all studied cases, the proposed controller gains initial values were: K_p = 7.315, K_i = 5.2409, and K_d = 2.394.

5.1. The Simple AVR Model Results

In this section, the validation of the proposed fuzzy EO PID controller is carried out through comparison with whale PID, whale PIDA [3], TLBO PIDA [17], and EO adaptive PI [35]. The comparison was first applied in a simple AVR model shown in Figure 1 with

reference 1 pu step signal. After that, without repeating the optimization, the comparison was carried out again with reference 0.8 and 1.2 pu step signal. Finally, the dynamic reference shown in Figure 7 is applied and a comparison was carried out again. Results of the simple AVR model and different references are shown in Figures 8–13.

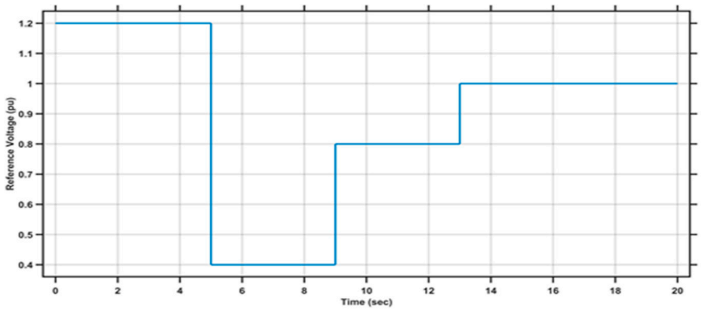


Figure 7. Dynamic reference.

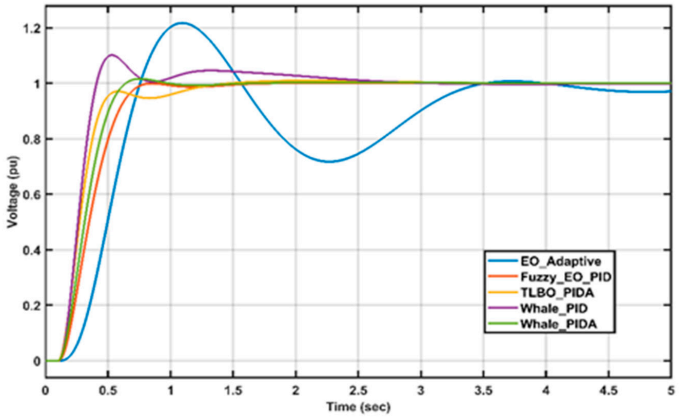


Figure 8. 1 pu step voltage reference for simple AVR model.

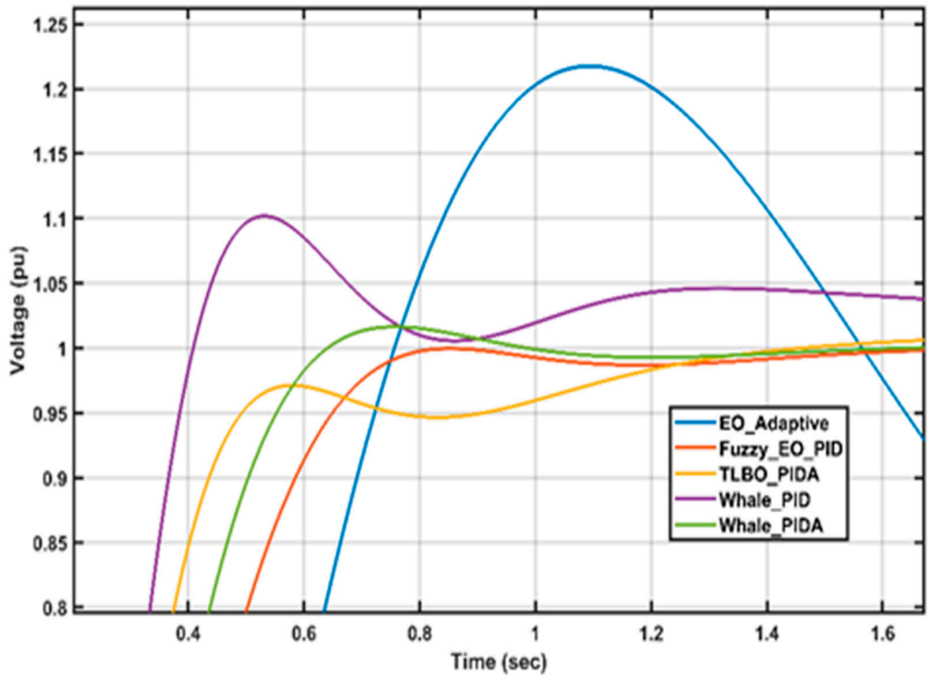


Figure 9. Focusing on the 1 pu step voltage reference case.

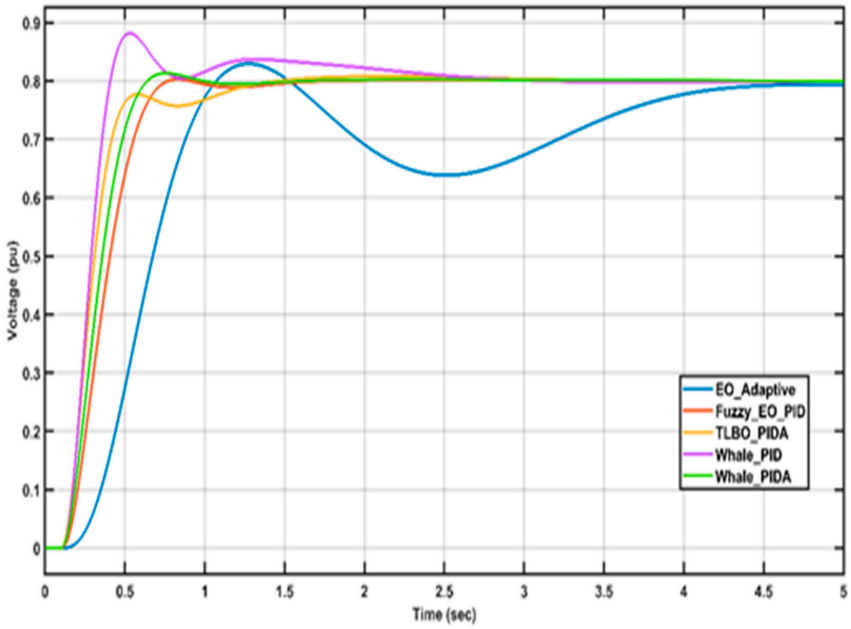


Figure 10. 0.8 pu step voltage reference for simple AVR model.

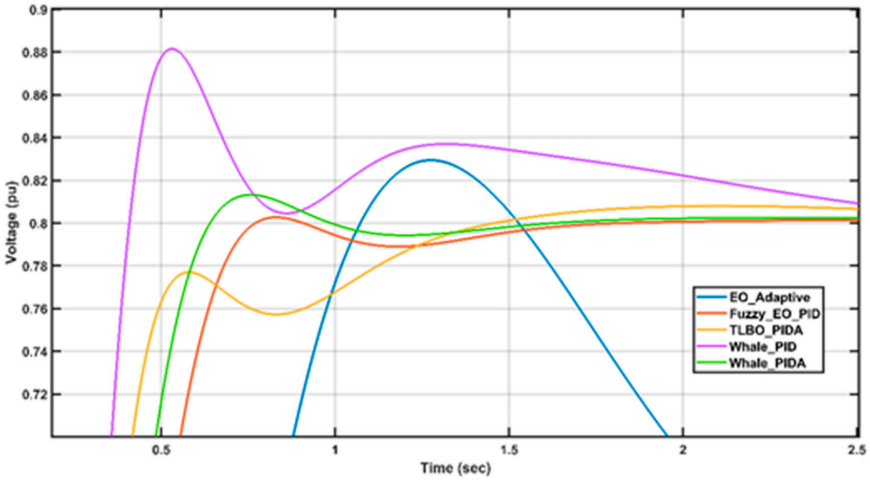


Figure 11. Focusing on the 0.8 pu step voltage reference case.

From Figures 8–13, it is clear that with references 0.8, 1, and 1.2 pu, the proposed controller had lower overshoot and settling time than whale PID, whale PIDA [3], TLBO PIDA [17], and EO adaptive PI [35] but with slightly slower response than a PIDA controller. Table 3 shows the voltage overshoot comparison between the proposed fuzzy EO PID controller against the other reported techniques for the simple AVR system at different step reference voltages.

Table 3. The voltage overshoot for the proposed fuzzy EO PID controller compared with the other techniques.

	1 pu Step Reference	0.8 pu Step Reference	1.2 pu Step Reference
EO adaptive	1.22 pu	0.825 pu	1.68 pu
TLBO PIDA	0.97 pu	0.778 pu	1.16 pu
Whale PID	1.1 pu	0.88 pu	1.32 pu
Whale PIDA	1.02 pu	0.815 pu	1.22 pu
Fuzzy EO PID	**1.0 pu**	**0.802 pu**	**1.2 pu**

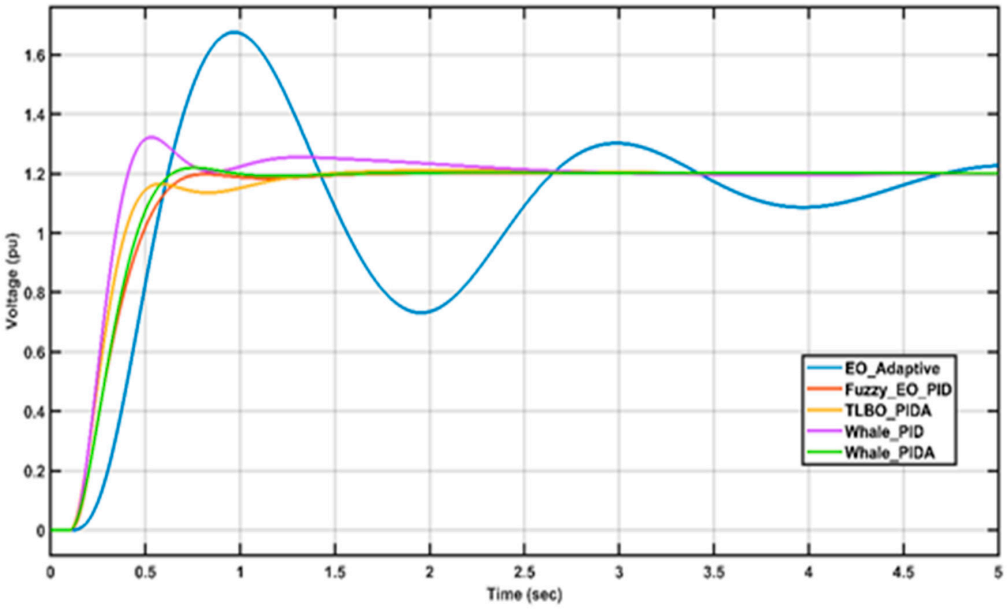


Figure 12. 1.2 pu step voltage reference for simple AVR model.

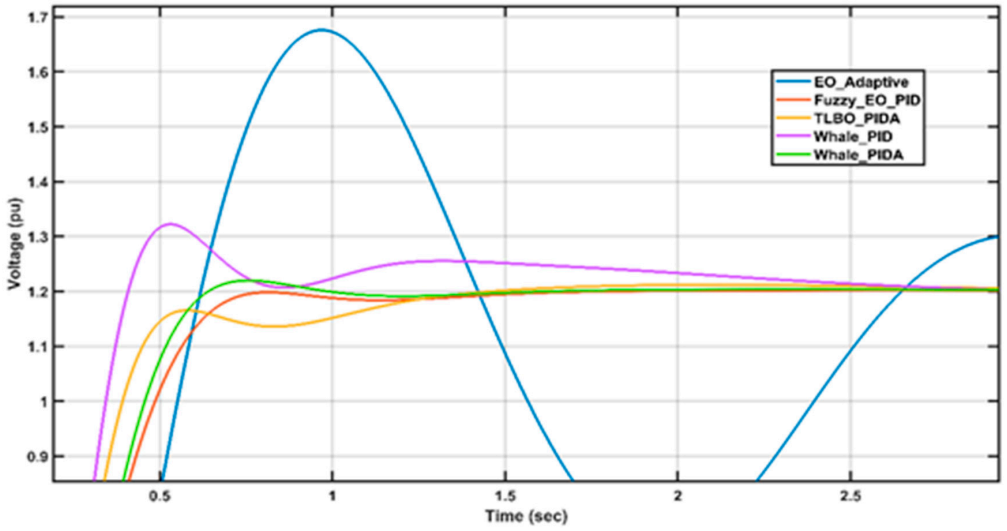


Figure 13. Focusing on 1.2 pu step voltage reference case.

From Table 3, in case of 1 pu step reference, the proposed fuzzy EO PID controller reduced the overshoot by 22% compared with EO adaptive, 10% compared with whale PID, 2% compared with whale PIDA and 3% compared with TLBO PIDA. In the case of 0.8 pu step reference, the fuzzy EO PID controller reduced the overshoot by 2.7% compared with EO adaptive, 8.8% compared with whale PID, 1% compared with whale PIDA and 3% compared with TLBO PIDA. In the case of 1.2 pu step reference, the fuzzy EO PID controller reduced the overshoot by 28.5% compared with EO adaptive, 9% compared with whale PID, 1.6% compared with whale PIDA and 3.5% compared with TLBO PIDA.

From the dynamic reference case results shown in Figures 14–16, the proposed fuzzy EO PID tracked the reference smoother than other controllers with lower settling time and overshoot but still had a slightly higher rising time than the PIDA controller.

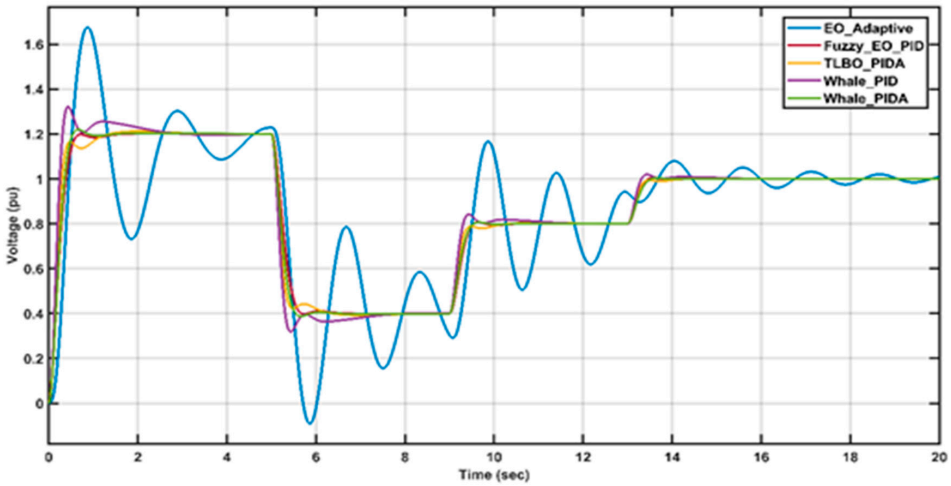


Figure 14. Dynamic voltage reference for simple AVR model.

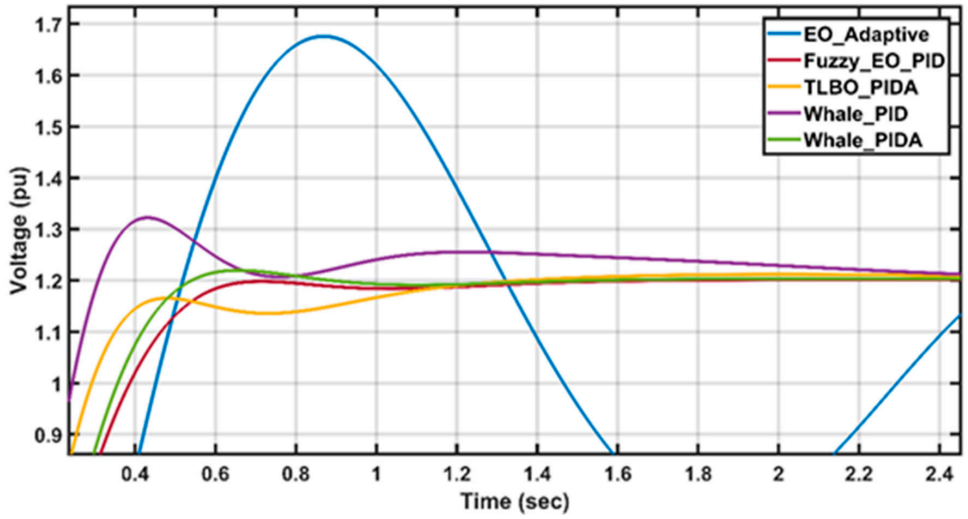


Figure 15. Focusing part 1 on the dynamic reference case.

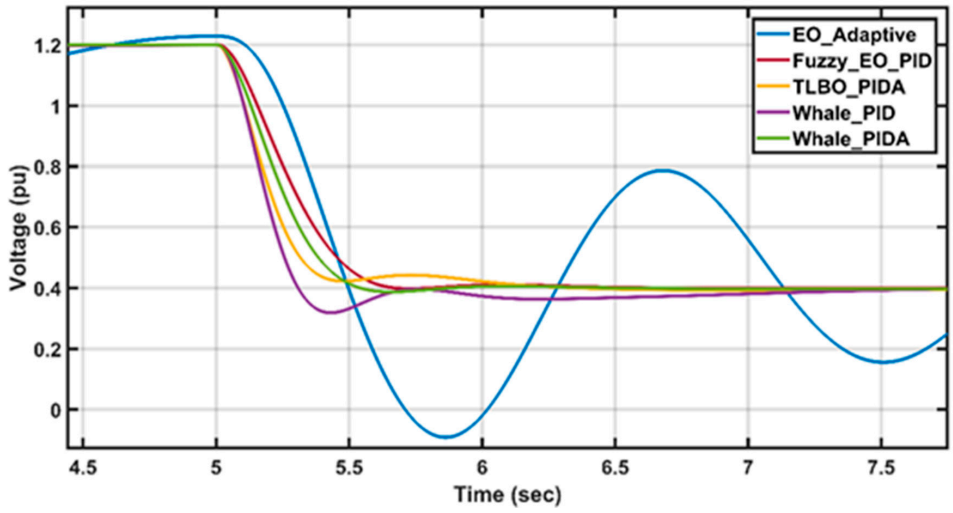


Figure 16. Focusing part 2 on the dynamic reference case.

5.2. Kundur System Results

In this section, the proposed fuzzy EO PID controller was used with the Kundur four-machines system without repeating the optimization. The proposed controller was inserted in all generators' excitation systems instead of its default lead–lag controller. The response of the proposed controller was compared with the default controller and the improved PSS system proposed in [36] as shown in Figures 17–19.

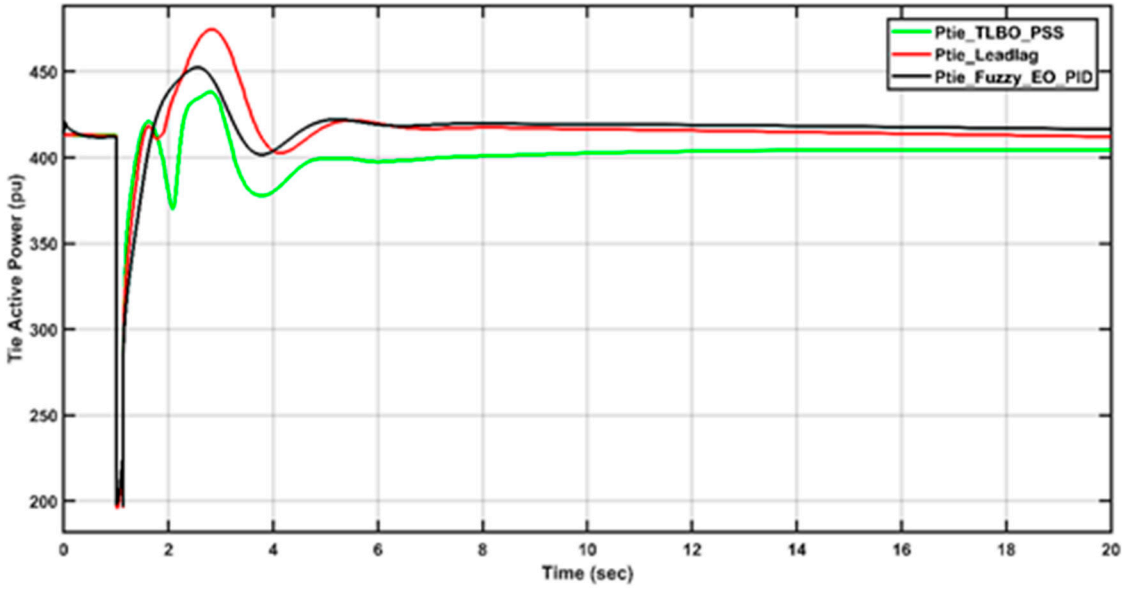


Figure 17. Tie power results for Kundur system.

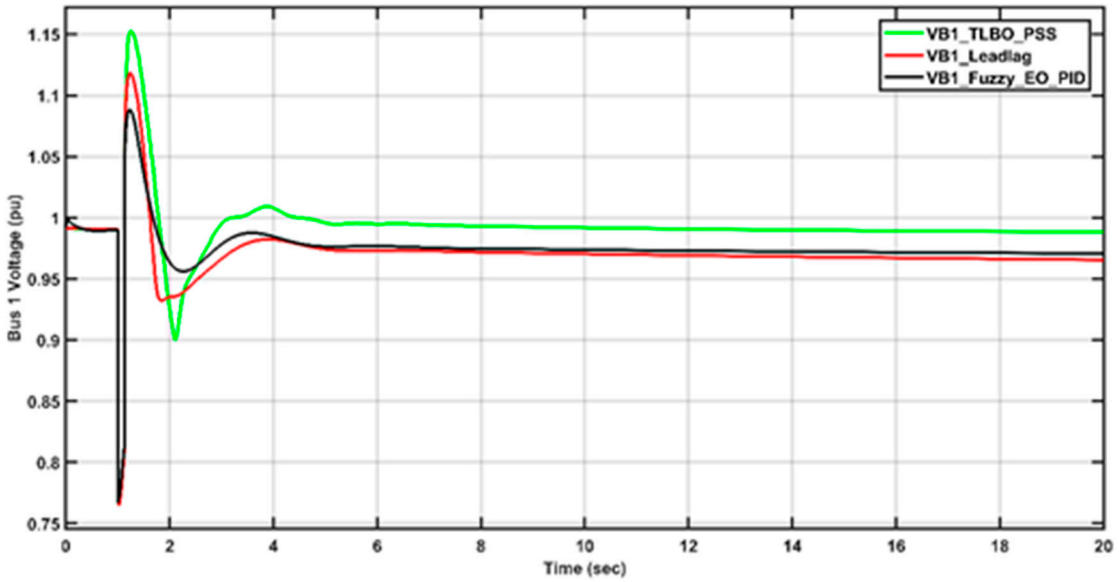


Figure 18. Bus 1 voltage results for Kundur system.

From Figure 17, the proposed controller had a smoothing Ptie response compared with the default controller and the modified PSS [36]. While from Figure 18, the voltage at bus 1 had an overshoot of around 1.07 pu in the proposed controller, 1.15 pu in the default controller, and 1.12 pu in the modified PSS case. Moreover, the steady-state voltage was around 0.98 pu in the case of the proposed controller and the modified PSS. Finally, the proposed controller had a smoother response in Bus 2 voltage waveform as shown in

Figure 19, with an also lower overshoot of around 1.06 pu compared with 1.1 pu in default and modified PSS.

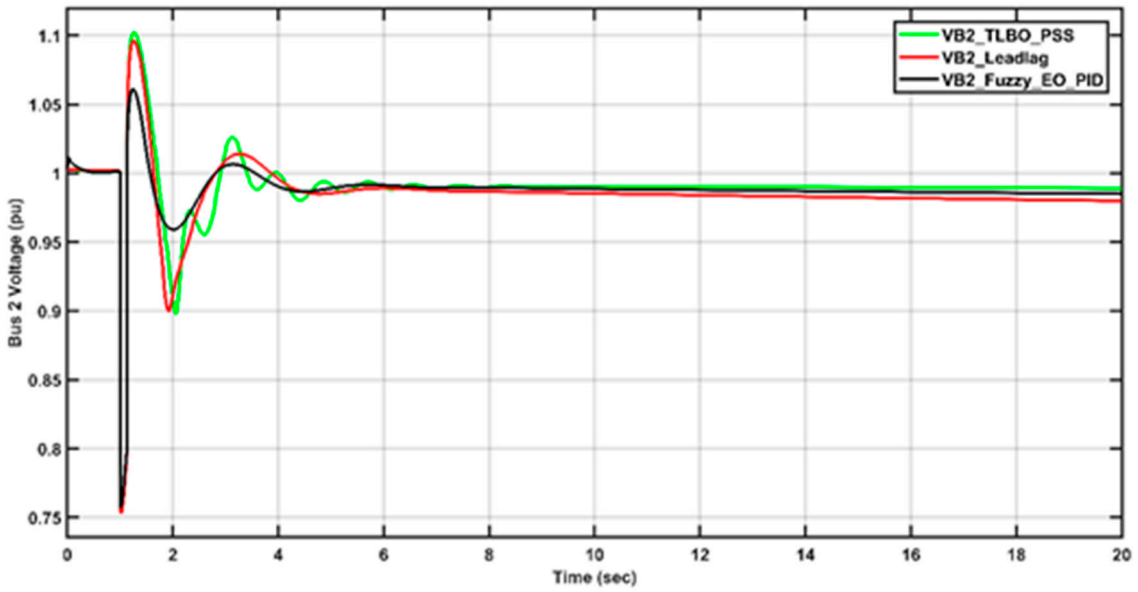


Figure 19. Bus 2 voltage results for Kundur system.

5.3. IEEE 9 Bus System

In this section, the proposed fuzzy EO PID controller was used with the IEEE 9-bus system, with three generators and three connected loads [29]. The proposed controller was inserted in both generators at buses 2 and 3 of the IEEE 9-bus system. The response of the proposed controller was compared with the default controller available. First, the normal operation was considered for the studied system. The bus 2 and 3 voltage waveforms are shown in Figures 20 and 21, respectively.

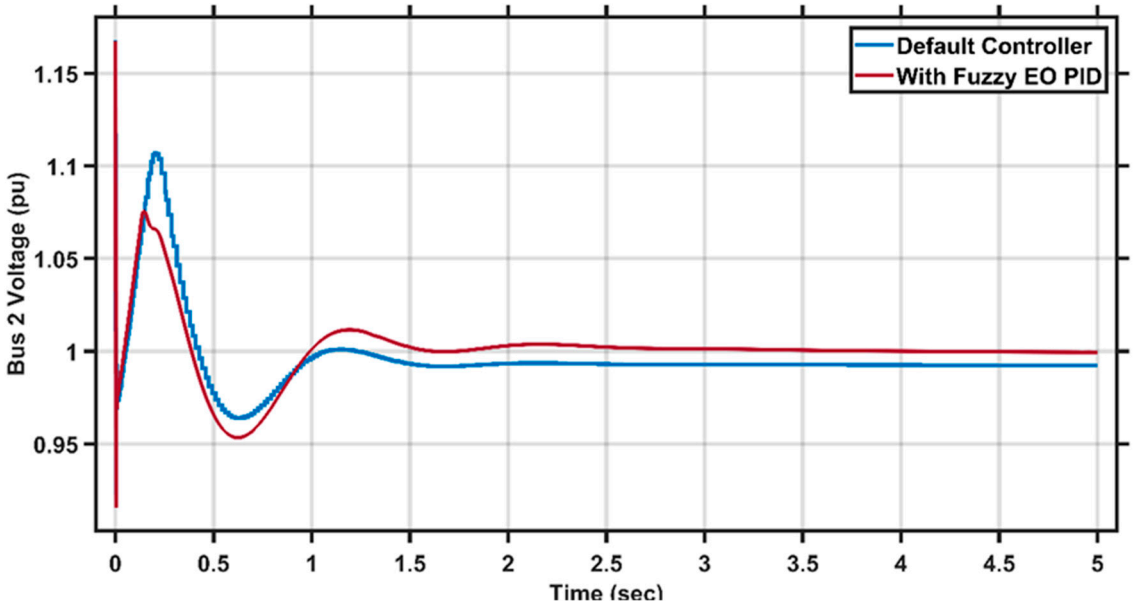


Figure 20. Bus 2 voltage at normal operation for the IEEE 9-bus system.

It can be seen that the performance of the proposed fuzzy EO PID controller was superior to the default controller, with lower voltage overshoot at both buses 2 and 3 by a 4.5% reduction for both buses compared with the default controller, and also with an accurate steady-state voltage of 1 pu.

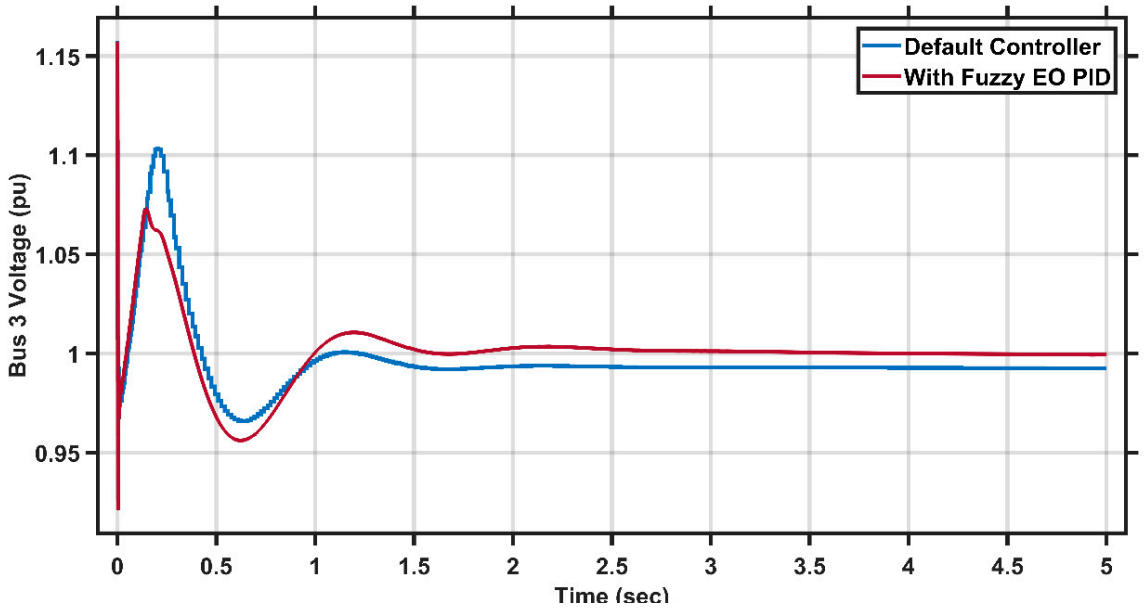


Figure 21. Bus 3 voltage at normal operation for the IEEE 9-bus system.

Second, the proposed controller performance was tested with an LG fault after lines 5–9 at bus 5 at 5 s and cleared at 5.3 s. The bus 2 and 3 voltage waveforms at faulty conditions are shown in Figures 22 and 23, respectively.

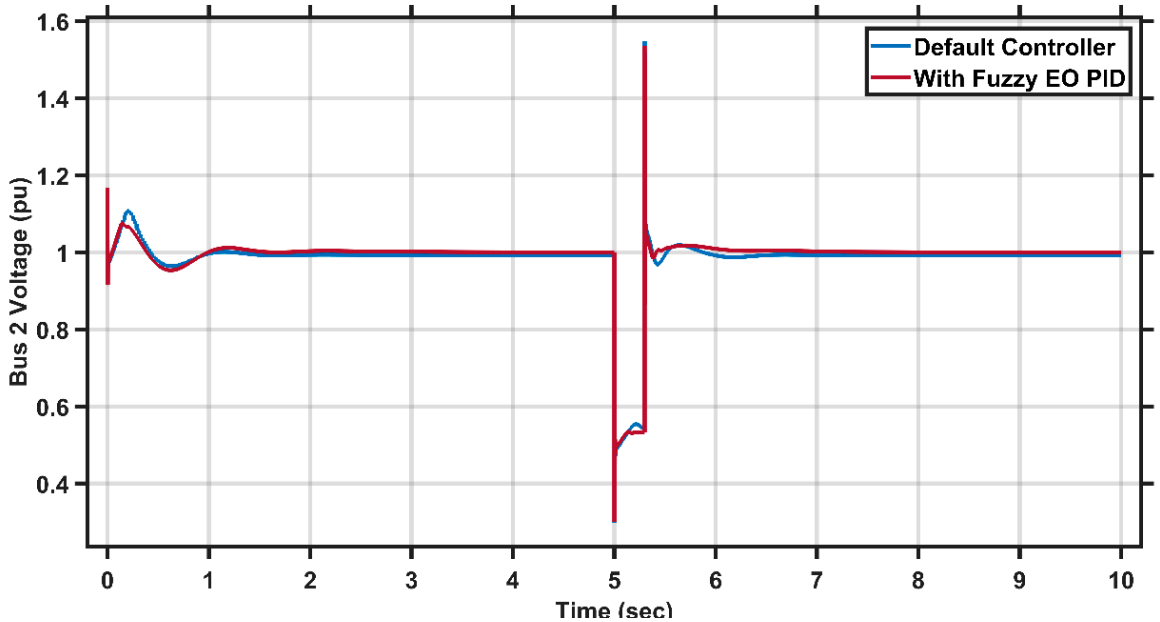


Figure 22. Bus 2 voltage at faulty condition for the IEEE 9-bus system.

It is evident from both Figures that the performance of the proposed fuzzy EO PID controller was superior to the default controller, with lower voltage overshoot and settling time at both buses 2 and 3.

Then, the proposed controller performance was tested when a dynamic loading condition was applied. At bus 8, a sudden load of 200 MW and 70 MVAr was added at 5 s, then 50% of the additional load was removed at 8 s, then the remaining 50% was removed at 10 s. The bus 2 and 3 voltage waveforms at dynamic loading conditions are shown in Figures 24 and 25, respectively. It is evident from both figures that the performance of the

proposed fuzzy EO PID controller was superior to the default controller, with a higher steady state voltage at both buses 2 and 3.

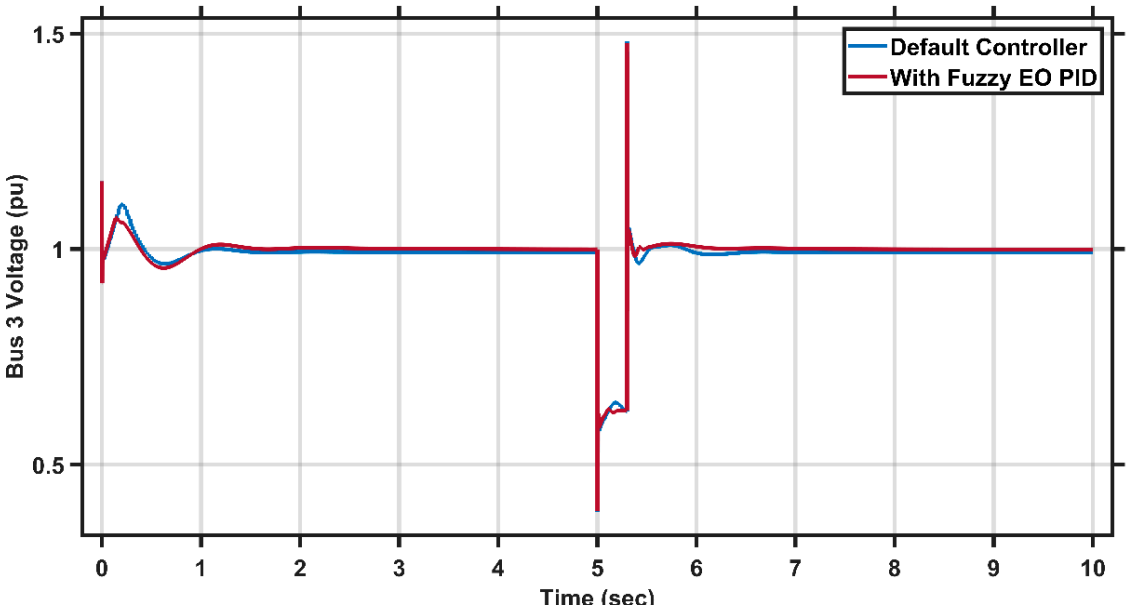


Figure 23. Bus 3 voltage at faulty condition for the IEEE 9-bus system.

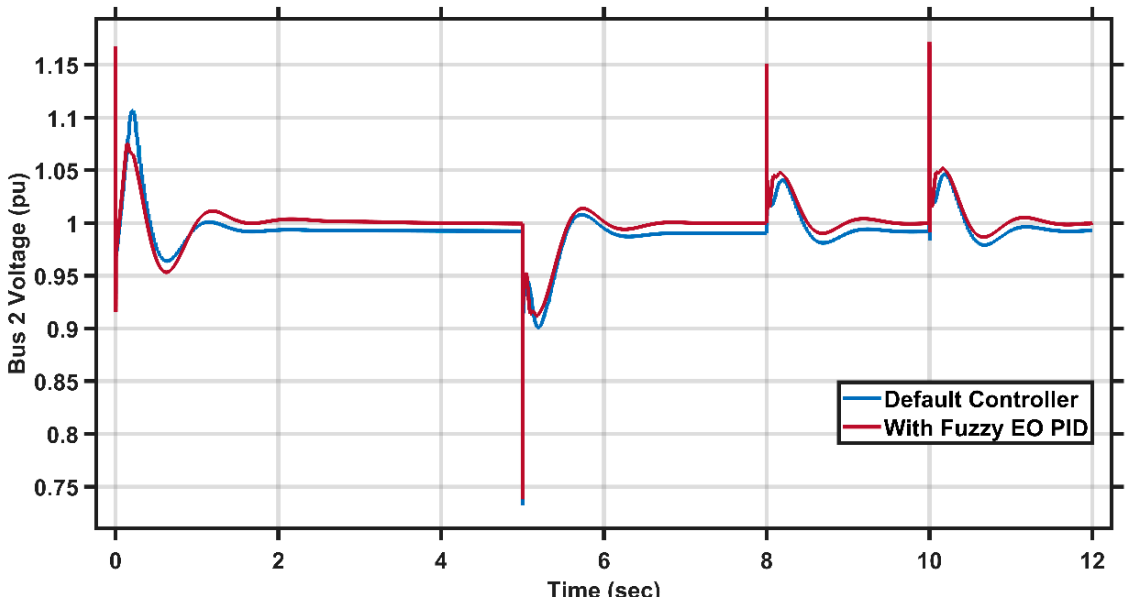


Figure 24. Bus 2 voltage at dynamic loading condition for the IEEE 9-bus system.

Finally, the proposed controller performance was tested when the system was islanded or disconnected from the infinite bus network at bus 4. Line 4–6 was first disconnected at 11 s, and then line 4–5 was disconnected at 13 s. The IEEE 9-bus system was then fully islanded between 13 s and 16 s. Then, line 4–6 was reconnected at 16 s and after that, line 4–5 was reconnected at 18 s. The bus 2 and 3 voltage waveforms in islanded operation are shown in Figures 26 and 27, respectively. As seen in both figures, the proposed controller was able to keep the voltage at around 0.92 pu when the system was fully islanded between 13 and 16 s and regained the 1 pu again when the system was restored to its original conditions.

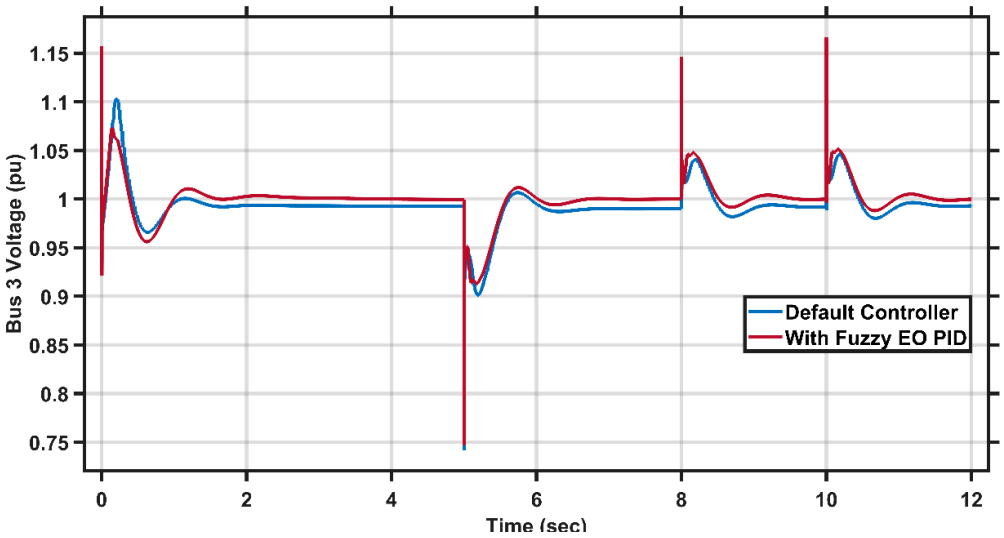


Figure 25. Bus 3 voltage at dynamic loading condition for the IEEE 9-bus system.

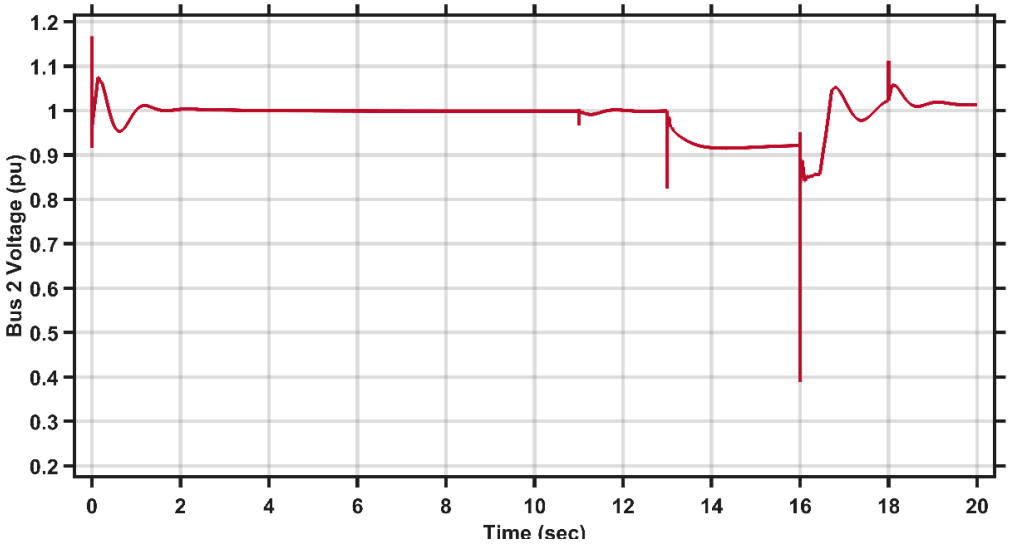


Figure 26. Bus 2 voltage at islanded operation for the IEEE 9-bus system.

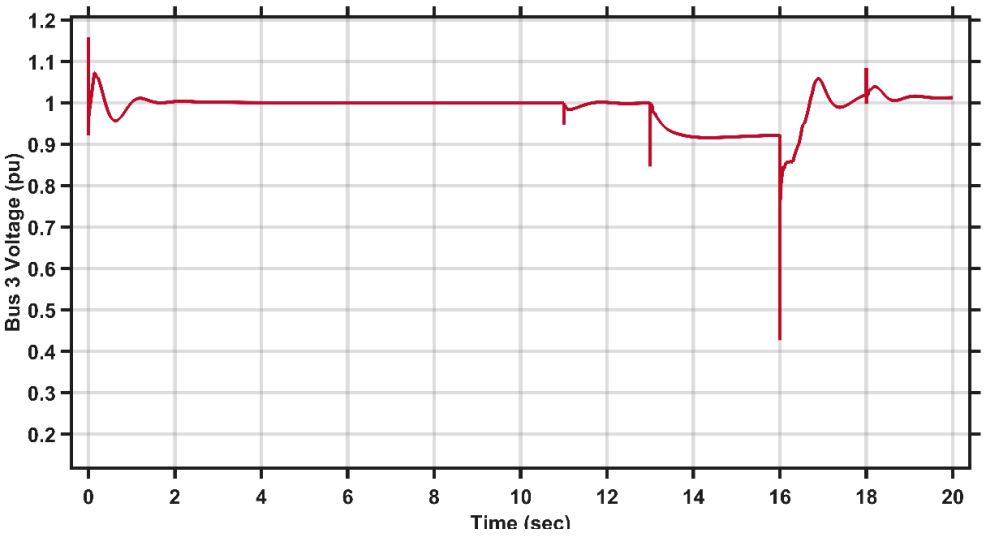


Figure 27. Bus 3 voltage at islanded operation for the IEEE 9-bus system.

From the previous testing condition of the IEEE 9-bus system, the robustness of the proposed fuzzy EO PID was proven and the superiority over the default controller is shown.

6. Conclusions

This paper proposed an auto-tuned fuzzy EO PID controller to enhance the AVR system performance. The gains of the controller were initialized by using EO optimization. The validation of the proposed controller was proven through three case studies. First, the proposed controller was applied to a simple AVR model under fixed and variable references. The results showed the superiority of the proposed controller in reducing the voltage overshoot by 10% compared with the PID, 28% compared with adaptive PID, and 3% compared with PIDA. Then, the proposed fuzzy EO PID controller was applied to the Kundur two-area system and compared with the default lead–lag controller and the improved PSS system in the literature and showed better dynamic performance through a reduction of voltage overshoot by 7% and 4%, respectively. Finally, the proposed controller was applied to the IEEE 9-bus system under normal, faulty, dynamic loading conditions, and compared with the default system controller, with superiority in overshoot reduction by 4.5%. Moreover, a smooth transition between the islanding and grid-connected modes of operation in the IEEE 9-bus system was obtained by the proposed controller.

Author Contributions: Conceptualization, S.M. and M.A.S.; Data curation, A.O.B. and M.A.A.; Formal analysis, A.O.B. and M.A.A.; Funding acquisition, M.A.S.; Investigation, A.O.B., S.M. and M.A.A.; Methodology, M.A.A.; Project administration, M.A.A.; Resources, S.M. and M.A.S.; Software, A.O.B.; Supervision, M.A.A.; Validation, M.A.A.; Visualization, S.M., M.A.S. and M.A.A.; Writing–original draft, S.M. and M.A.S.; Writing–review & editing, M.A.S. and M.A.A. All authors have read and agreed to the published version of the manuscript.

Funding: This research was funded by Future University in Egypt (FUE), grant number 2000$ and The APC was funded by Future University in Egypt (FUE).

Data Availability Statement: The study did not report any data.

Conflicts of Interest: The authors declare no conflict of interest.

References

1. Çelik, E.; Durgut, R. Performance enhancement of automatic voltage regulator by modified cost function and symbiotic organisms search algorithm. *Eng. Sci. Technol. Int. J.* **2018**, *21*, 1104–1111. [CrossRef]
2. Mohanty, P.K.; Sahu, B.K.; Panda, S. Tuning and Assessment of Proportional–Integral–Derivative Controller for an Automatic Voltage Regulator System Employing Local Unimodal Sampling Algorithm. *Electr. Power Compon. Syst.* **2014**, *42*, 959–969. [CrossRef]
3. Mosaad, A.M.; Attia, M.A.; Abdelaziz, A.Y. Comparative Performance Analysis of AVR Controllers Using Modern Optimization Techniques. *Electr. Power Compon. Syst.* **2018**, *46*, 2117–2130. [CrossRef]
4. Ali, M.N.; Soliman, M.; Mahmoud, K.; Guerrero, J.M.; Lehtonen, M.; Darwish, M.M.F. Resilient Design of Robust Multi-Objectives PID Controllers for Automatic Voltage Regulators: D-Decomposition Approach. *IEEE Access* **2021**, *9*, 106589–106605. [CrossRef]
5. Köse, E. Optimal Control of AVR System with Tree Seed Algorithm-Based PID Controller. *IEEE Access* **2020**, *8*, 89457–89467. [CrossRef]
6. Dogruer, T.; Can, M.S. Design and robustness analysis of fuzzy PID controller for automatic voltage regulator system using genetic algorithm. *Trans. Inst. Meas. Control* **2022**, *44*, 1862–1873. [CrossRef]
7. Modabbernia, M.; Alizadeh, B.; Sahab, A.; Moghaddam, M.M. Robust control of automatic voltage regulator (AVR) with real structured parametric uncertainties based on H∞ and μ-analysis. *ISA Trans.* **2020**, *100*, 46–62. [CrossRef]
8. Gaing, Z.-L. A particle swarm optimization approach for optimum design of PID controller in AVR system. *IEEE Trans. Energy Convers.* **2004**, *19*, 384–391. [CrossRef]
9. Rahimian, M.S.; Raahemifar, K. Optimal PID controller design for AVR system using particle swarm optimization algorithm. In Proceedings of the 2011 24th Canadian Conference on Electrical and Computer Engineering (CCECE), Niagara Falls, ON, Canada, 8–11 May 2011; pp. 000337–000340.
10. Ekinci, S.; Hekimoglu, B. Improved kidney-inspired algorithm approach for tuning of PID controller in AVR system. *IEEE Access* **2019**, *7*, 39935–39947. [CrossRef]
11. Zeng, G.-Q.; Chen, J.; Dai, Y.-X.; Li, L.-M.; Zheng, C.-W.; Chen, M.-R. Design of fractional order PID controller for automatic regulator voltage system based on multi-objective extremal optimization. *Neuro Comput.* **2015**, *160*, 173–184. [CrossRef]

12. Bingul, Z.; Karahan, O. A novel performance criterion approach to optimum design of PID controller using cuckoo search algorithm for AVR system. *J. Frankl. Inst.* **2018**, *355*, 5534–5559. [CrossRef]
13. Razmjooy, N.; Khalilpour, M.; Ramezani, M. A new meta-heuristic optimization algorithm inspired by FIFA world cup competitions: Theory and its application in PID designing for AVR system. *J. Control Autom. Electr. Syst.* **2016**, *27*, 419–440. [CrossRef]
14. Tang, Y.; Cui, M.; Hua, C.; Li, L.; Yang, Y. Optimum design of fractional order PID controller for AVR system using chaotic ant swarm. *Expert Syst. Appl.* **2012**, *39*, 6887–6896. [CrossRef]
15. Pan, I.; Das, S. Frequency domain design of fractional order PID controller for AVR system using chaotic multi-objective optimization. *Int. J. Electr. Power Energy Syst.* **2013**, *51*, 106–118. [CrossRef]
16. Ayas, M.S. Design of an optimized fractional high-order differential feedback controller for an AVR system. *Electr. Eng.* **2019**, *101*, 1221–1233. [CrossRef]
17. Mosaad, A.M.; Attia, M.A.; Abdelaziz, A.Y. Whale optimization algorithm to tune PID and PIDA controllers on AVR system. *Ain Shams Eng. J.* **2019**, *10*, 755–767. [CrossRef]
18. Mokeddem, D.; Mirjalili, S. Improved whale optimization algorithm applied to design PID plus second-order derivative controller for automatic voltage regulator system. *J. Chin. Inst. Eng.* **2020**, *43*, 541–552. [CrossRef]
19. Chatterjee, S.; Mukherjee, V. PID controller for automatic voltage regulator using teaching–learning based optimization technique. *Int. J. Electr. Power Energy Syst.* **2016**, *77*, 418–429. [CrossRef]
20. Micev, M.; C'alasan, M.; Oliva, D. Design and robustness analysis of an Automatic Voltage Regulator system controller by using Equilibrium Optimizer algorithm. *Comput. Electr. Eng.* **2021**, *89*, 106930. [CrossRef]
21. Elsisi, M.; Soliman, M. Optimal design of robust resilient automatic voltage regulators. *ISA Trans.* **2021**, *108*, 257–268. [CrossRef]
22. Shayeghi, H.; Younesi, A.; Hashemi, Y. Optimal design of a robust discrete parallel FP+FI+FD controller for the Automatic Voltage Regulator system. *Int. J. Electr. Power Energy Syst.* **2015**, *67*, 66–75. [CrossRef]
23. Priyambada, S.; Sahu, B.K.; Mohanty, P.K. Fuzzy-PID controller optimized TLBO approach on automatic voltage regulator. In Proceedings of the 2015 International Conference on Energy, Power and Environment: Towards Sustainable Growth (ICEPE), Shillong, India, 12–13 June 2015; pp. 1–6. [CrossRef]
24. Shabib, G. Implementation of a discrete fuzzy PID excitation controller for power system damping. *Ain Shams Eng. J.* **2012**, *3*, 123–131. [CrossRef]
25. Mukherjee, V.; Ghoshal, S. Intelligent particle swarm optimized fuzzy PID controller for AVR system. *Electr. Power Syst. Res.* **2007**, *77*, 1689–1698. [CrossRef]
26. Panda, M.K.; Pillai, G.N.; Kumar, V. Design of an interval type-2 fuzzy logic controller for automatic voltage regulator system. *Electr. Power Compon. Syst.* **2011**, *40*, 219–235. [CrossRef]
27. Kundur, P.S.; Malik, O.P. *Power System Stability and Control*; McGraw-Hill Professional: New York, NY, USA, 1994; pp. 813–816. ISBN 007035958X/9780070359581.
28. Baltensperger, D.; Dobrowolski, J.; Obushevs, A.; Sevilla, F.R.S.; Korba, P. Scaling Version of Kundur's Two-Areas System for Electromechanical Oscillations Representation. In Proceedings of the 2020 International Symposium on Power Electronics, Electrical Drives, Automation and Motion (SPEEDAM), Sorrento, Italy, 24–26 June 2020; pp. 243–249. [CrossRef]
29. Anderson, P.M.; Fouad, A.A. *Power System Control and Stability*; Iowa State University Press: Ames, Iowa, 1977.
30. Jäkel, J.; Mikut, R.; Bretthauer, G. *Fuzzy Control Systems*; Institute of Applied Computer Science, Forschungszentrum Karlsruhe GmbH: Leipzig, Germany, 2004.
31. Farouk, N.; Bingqi, T. Application of self-tuning fuzzy PID controller on the AVR system. In Proceedings of the 2012 IEEE International Conference on Mechatronics and Automation, Chengdu, China, 5–8 August 2012; pp. 2510–2514. [CrossRef]
32. Vasanthi, S.; Gopila, M.; Gnanambal, I. Fuzzy and PID Excitation CONTROL System with AVR in Power System Stability Analysis. *Int. J. Eng. Adv. Technol.* **2012**, *1*, 2249–8958.
33. Mansour, S.; Badr, A.O.; Attia, M.A.; Sameh, M.A.; Kotb, H.; Elgamli, E.; Shouran, M. Fuzzy Logic Controller Equilibrium Base to Enhance AGC System Performance with Renewable Energy Disturbances. *Energies* **2022**, *15*, 6709. [CrossRef]
34. Faramarzi, A.; Heidarinejad, M.; Stephens, B.; Mirjalili, S. Equilibrium optimizer: A novel optimization algorithm. *Knowl. Based Syst.* **2020**, *191*, 105190. [CrossRef]
35. Attia, M.A.; Abdelaziz, A.Y.; Sarita, K.; Vardhan, A.S.S.; Vardhan, A.S.S.; Singh, S.; Saket, R.K. AVR Performance Enhancement by Using Adaptive PI Controller. In Proceedings of the Third International Conference on Intelligent Computing, Information and Control Systems, Trichy, India, 2–3 July 2021; Springer: Singapore, 2022; pp. 249–260.
36. Yakout, A.H.; Mahmoud, A.A. Damping Inter-Area Oscillations Via Weighted Area Signals to PSSs Using TLBO & HS Algorithm. In Proceedings of the 2019 21st International Middle East Power Systems Conference (MEPCON), Cairo, Egypt, 17–19 December 2019; IEEE: Piscatway, NJ, USA, 2020; pp. 496–501.